Protein Science (1999), *8*:2655–2662. Cambridge University Press. Printed in the USA.

The mechanism of aconitase: 1.8 Å resolution crystal structure of the S642A:citrate complex

S.J. LLOYD, H. LAUBLE,[1] G.S. PRASAD, AND C.D. STOUT

Department of Molecular Biology, The Scripps Research Institute, 10550 North Torrey Pines Road, La Jolla, California 92037

(RECEIVED August 16, 1999; ACCEPTED October 6, 1999)

Abstract

The crystal structure of the S642A mutant of mitochondrial aconitase (mAc) with citrate bound has been determined at 1.8 Å resolution and 100 K to capture this binding mode of substrates to the native enzyme. The 2.0 Å resolution, 100 K crystal structure of the S642A mutant with isocitrate binding provides a control, showing that the Ser → Ala replacement does not alter the binding of substrates in the active site. The aconitase mechanism requires that the intermediate product, *cis*-aconitate, flip over by 180° about the Cα–Cβ double bond. Only one of these two alternative modes of binding, that of the isocitrate mode, has been previously visualized. Now, however, the structure revealing the citrate mode of binding provides direct support for the proposed enzyme mechanism.

Keywords: aconitase mechanism; active site mutants; crystal structures

Aconitase [citrate (isocitrate) hydroxylase, E.C. 4.2.1.3.] employs a [4Fe-4S] cluster to catalyze the stereospecific dehydration-rehydration of citrate to isocitrate via *cis*-aconitate in the tricarboxylic acid cycle. The heart mitochondrial enzyme has been extensively characterized by crystallographic, biochemical, spectroscopic, and kinetic methods (Kennedy & Stout, 1992; Beinert et al., 1996), providing a model system for understanding the role of [Fe-S] clusters in nonredox reactions. Other isomerase enzymes also contain [Fe-S] clusters involved in catalysis (Skala et al., 1991; Flint & Allen, 1996; Flint et al., 1993). DNA and RNA binding regulatory proteins, such as the *Escherichia coli* FNR protein (Lazazzera et al., 1996; Khoroshilova et al., 1997) and cytosolic aconitase, the iron regulatory protein (IRP) (Rouault et al., 1991; Haile et al., 1992), contain [Fe-S] clusters. In these cases, the protein and [Fe-S] cluster structure are altered in response to cellular oxidants or iron levels (Beinert & Kiley, 1996; Green et al., 1996; Rouault & Klausner, 1996).

Crystallographic and spectroscopic studies of mitochondrial aconitase (mAc) have defined the [Fe-S] cluster structure in the several states of the enzyme arising from cluster transformations and interactions with substrates, inhibitors, and solvent species (Beinert et al., 1996). The application of isotopic labeling of the substrate, inhibitor, and solvent atoms in Mössbauer, EPR, and ENDOR experiments, in combination with crystal structures, kinetics, the use of reaction intermediate analogs, and site-directed mutagenesis has led to a mechanism for the multiple step reaction catalyzed (Schloss et al., 1984; Emptage, 1988; Lauble et al., 1992; Zheng et al., 1992) (Fig. 1). First, the prochiral substrate citrate binds stereospecifically and is dehydrated, forming the stable intermediate *cis*-aconitate. For the reaction to proceed, the mechanism requires that *cis*-aconitate be released from the enzyme and rebind with the positions of its Cα and Cβ atoms inverted. Kinetically, this step may involve displacement by a second molecule of *cis*-aconitate in the inverted configuration; the net effect is to flip this substrate by 180° about the Cα–Cβ double bond. Reversal of the chemical steps results in rehydration of *cis*-aconitate to form (2R,3S) isocitrate. The configurations of *cis*-aconitate are termed citrate-mode and isocitrate-mode (Fig. 1). In this paper, site-directed mutagenesis is used to capture the citrate mode, implied by the mechanism but not previously visualized.

Mitochondrial aconitase is a single polypeptide (M_r 83 kD) (Zheng et al., 1990); three cysteines ligate to a [3Fe-4S] cluster that in turn incorporates a fourth Fe upon activation. This Fe (Fe4) interacts with substrate carboxyl and hydroxyl oxygen atoms and solvent species. High-resolution structures have been obtained for the substrate free enzyme and for the enzyme in complex with isocitrate and inhibitors (Beinert et al., 1996). Because the native enzyme preferentially crystallizes with bound isocitrate, it has not been possible to prepare crystals with bound citrate or *cis*-aconitate (Lauble et al., 1992). In the model (Fig. 1), the *cis*-aconitate complex in the isocitrate mode is derived by analogy with the *trans*-aconitate complex (Lauble et al., 1994). Similarly, the *cis*-aconitate model in the citrate mode is derived by analogy with the *trans*-aconitate and nitrocitrate complexes. Finally, the model for citrate is also based on the nitrocitrate complex. However, in this case, nitrocitrate is weakly bound, being only 75% occupied in compe-

Reprint requests to: C.D. Stout, Department of Molecular Biology, The Scripps Research Institute, 10550 North Torrey Pines Road, La Jolla, California 92037; e-mail: dave@scripps.edu.

[1] Present address: Max Delbruck Centrum für Molekuläre Medizin, Robert Roessle Strasse 10, 13125 Berlin, Germany.

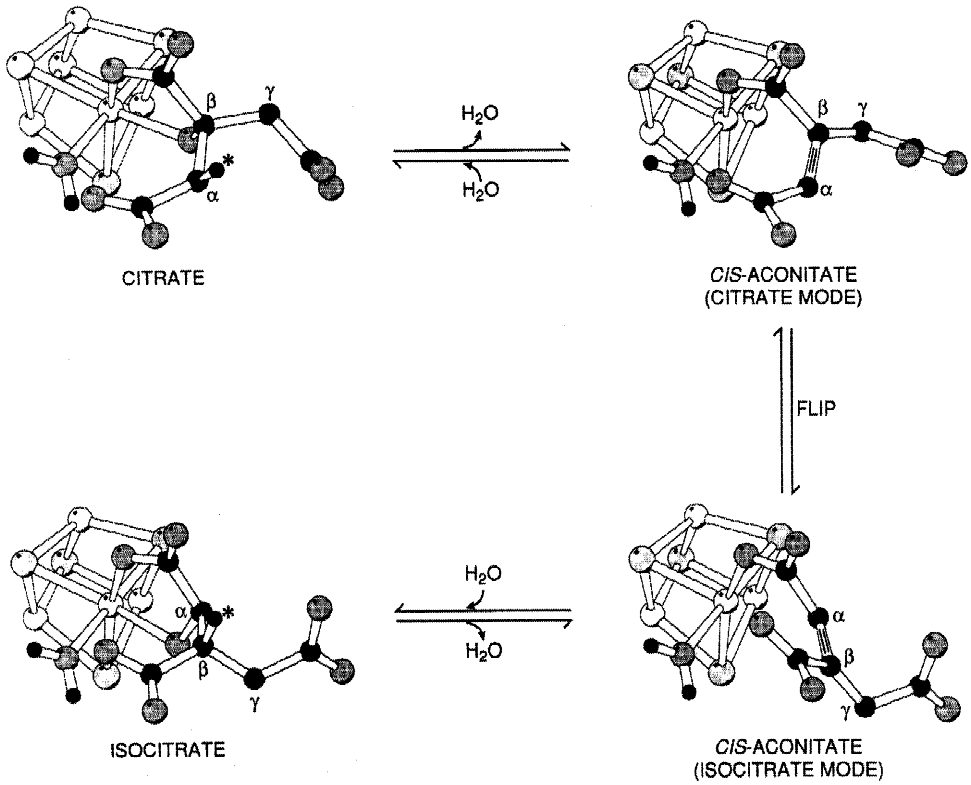

Fig. 1. Model for the mechanism of the reaction catalyzed by aconitase. Only one of the four states depicted corresponds to a previously determined crystal structure, that of the isocitrate complex. In this paper direct structural evidence for the existence of the citrate complex is presented, and the isocitrate complex is independently confirmed. The intermediate product, *cis*-aconitate, is proposed to bind in two ways related by 180° rotation about Cα–Cβ double bond. The asterisk denotes the proton that is stereospecifically abstracted from citrate and replaced in isocitrate. Hydrogen atoms on the H_2O molecule bound to the unique Fe (Fe4) of the [4Fe-4S] cluster are also depicted. Atoms are shaded: white, Fe; light gray, S; dark gray, O; black, C and H. This figure is reprinted from Lauble et al. (1994).

tition with 25% occupancy by sulfate (Lauble et al., 1994). Further, the Fe4-oxygen distances in the nitrocitrate complex are long, 2.8–3.3 Å, but Mössbauer results indicate that citrate must interact strongly with Fe4 (Kent et al., 1985). Therefore, the nitrocitrate complex does not directly confirm the existence of the citrate mode.

The S642A mutant was chosen for structural analysis based on kinetic and EPR properties. It has a reduced V_{max} but only slightly elevated K_m and exhibits native-like interaction of citrate with the [4Fe-4S] cluster (Zheng et al., 1992). Further, it is the slowest known mutant with V_{max} reduced by $1.8–8.7 \times 10^{-5}$ relative to the native enzyme. In the proposed mechanism Ser642 is the base, abstracting a proton from Cα of citrate (Cβ of isocitrate) (Fig. 1). Crystal structures of the citrate and isocitrate complexes of the S642A mutant are described, providing direct support for the citrate mode of binding.

Results and discussion

Crystal structures of the citrate and isocitrate complexes of S642A mAc have been refined at 1.8 and 2.0 Å resolution, respectively. The complexes were prepared by soaking crystals of this kinetically impaired mutant. In the S642A:isocitrate complex, the substrate binds in a manner very similar to that of isocitrate to the native enzyme, demonstrating that the Ser → Ala replacement has not otherwise altered the interactions of substrates within the active site. In the S642A:citrate complex citrate is directly coordinated to Fe4 of the [4Fe-4S] cluster via Cβ carboxyl and hydroxyl oxygen atoms. Consequently, the Cα–Cβ bond is inverted with respect to isocitrate, confirming the presence of the citrate mode in the mechanism.

Structure determination

The expression method previously reported (Zheng et al., 1992) was modified, and a purification scheme developed to improve the purity of the recombinant protein for crystallization (see Materials and methods). An additional Sephacryl-200 column step increased the time under aerobic conditions, resulting in partial loss of the [Fe-S] cluster; however, the cluster could be fully reconstituted (Kennedy & Beinert, 1988). Colloidal ferrous sulfide from the reconstitution reaction was removed using an Octyl-Sepharose column. Partial re-oxidation of the [Fe-S] cluster to the [3Fe-4S] form occurred during this step, but the enzyme was reactivated to the [4Fe-4S] form (Emptage et al., 1983) prior to anaerobic crystallization. Overall, recombinant mutant mAc could be prepared in good yield with sufficient purity to be crystallized using the established seeding procedure (Lauble et al., 1992).

Orthorhombic crystals of the S642A mutant were soaked in 40 mM solutions of citrate and isocitrate and flash-frozen at 100 K for data collection (Table 1). The structures were solved by molecular replacement using the structure of native mAc (Robbins & Stout, 1989) and were refined as described in Materials and methods (Table 1). The unbiased electron density at 1.8 Å resolution for the citrate soaked crystal, calculated prior to modeling any substrate species in the active site, reveals the orientation of bound citrate (Fig. 2A). The Cα and Cγ atoms linking their respective carboxyl groups to the central Cβ atom are resolved, as is the hydroxyl group attached to the Cβ atom of citrate. Similarly, unbiased electron density at 2.0 Å resolution for the isocitrate soaked crystal reveals the orientation of isocitrate (Fig. 2B). Therefore, the positions of the Cα and Cβ groups of citrate are interchanged with respect to isocitrate, consistent with the model for the binding modes of substrates to mAc (Fig. 1).

S642A:citrate complex

The structure of the S642A mutant of mAc with citrate binding is very similar to that of native mAc with isocitrate binding (Lauble et al., 1992) with no significant changes in the conformation of active site residues. The root-mean-square deviation (RMSD) of 753 Cα atoms following least-squares superposition of the two structures is 0.43 Å. Citrate is coordinated to Fe4 of the [4Fe-4S] cluster via a Cβ-carboxyl oxygen and the Cβ-hydroxyl group with Fe-O distances of 2.37 and 2.59 Å, respectively (Fig. 3), in accordance with the Mössbauer results (Kent et al., 1985). An H_2O molecule is coordinated to Fe4 (Fe-O distance 2.19 Å) making Fe4 six-coordinate with octahedral geometry. Fe4 in the isocitrate complex of native mAc has the same geometry with Fe-O distances of 2.49, 2.15, and 2.20 Å to carboxyl, hydroxyl, and H_2O oxygen atoms, respectively. Thus, the only significant difference in citrate vs. isocitrate coordination to Fe4 is the ~0.4 Å longer interaction with the hydroxyl group in the citrate complex. The binding of citrate in the active site involves the same 13 salt-bridging and hydrogen bonding interactions observed in the isocitrate complex of native mAc (Fig. 3). The similarity of the interactions for the two substrates is consistent with the role of the Ser642 as the base in the reaction, as substitution with Ala has not affected these interactions.

Table 1. *Data collection and refinement*

Mutant	S642A		S642A	
Complex	Citrate		Isocitrate	
Space group	$P2_12_12$		$P2_12_12$	
Unit cell, Å	176.1, 71.4, 71.8		176.4, 71.4, 71.9	
Total observations	285,614		219,481	
Unique reflections	82,013		63,472	
All data				
Resolution range (Å)	20.0–1.81		20.0–1.98	
Redundancy	3.5		3.5	
Completeness	99.0%		98.8%	
$I/\sigma(I)$	5.5		6.0	
$R_{symm}(I)$	0.071		0.108	
Last shell				
Resolution range (Å)	1.86–1.81		2.03–1.98	
Redundancy	2.4		2.4	
Completeness	88.1%		86.0%	
$I/\sigma(I)$	1.9		2.0	
$R_{symm}(I)$	0.372		0.368	
Refinement				
Resolution range (Å)	20.0–1.81		20.0–1.98	
No. of reflections $> 2.0\ \sigma_F$	75,071		62,380	
R-factor	0.211		0.212	
R_{free} for 5% of reflections	0.251		0.249	
RMSDs				
Bonds (Å)	0.019		0.019	
Angles (deg)	3.49		3.46	
Planes (deg)	1.39		1.54	
No. of atoms/avgerage *B* (Å^2)				
Protein	5,814	29.2	5,814	23.1
[4Fe-4S](OH_2)	9	25.4	9	26.4
Substrate	13	24.8	13	27.2
H_2O ($B < 70$ Å^2)	651	44.2	593	38.1
Total	6,487	—	6,429	—

S642A:isocitrate complex

The structure of the S642A mutant of mAc with isocitrate binding is also very similar to that of native mAc with isocitrate binding (Fig. 4A), and there are no significant changes in the conformation of active site residues. The RMSD of 753 Cα atoms following least-squares superposition of the two structures is 0.39 Å. Isocitrate is coordinated to Fe4 of the [4Fe-4S] cluster via a Cα-carboxyl oxygen and the Cα-hydroxyl group with Fe-O distances of 2.34 and 2.73 Å, respectively. An H_2O molecule is bound to six coordinate Fe4 with a Fe-O distance of 2.16 Å. All 13 hydrogen bonds observed for the complex of native mAc with isocitrate (and for the S642A:citrate complex) are observed for the S642A:isocitrate complex as well. Although the bound conformations of isocitrate are very similar, there is a small shift of isocitrate away from the [4Fe-4S] cluster in the mutant, resulting in an average displacement of 0.42 Å. This accounts for most of the ~0.6 Å longer Fe4-hydroxyl distance in the mutant complex. The shift may be due to the absence of the Ser642 hydroxyl group, which, as the proposed base in the reaction, has a short contact of 3.18 Å with Cβ of isocitrate (Fig. 4A). The shift of isocitrate in the mutant is essentially in the direction of residue 642. Nevertheless, the structure of the S642A:isocitrate complex shows that the Ser → Ala mutation has not altered the binding mode of isocitrate. Therefore, this mutation would not be expected to significantly affect the binding mode of citrate with respect to the native enzyme.

Citrate mode

The S642A:citrate complex is superposed onto the isocitrate complex of native mAc in Figure 4B to show how the two substrates bind with their Cα–Cβ bonds inverted with respect to each other. Nevertheless, they coordinate to Fe4 in the same manner and participate in all of the same interactions within the active site. The nine atoms of the isosteric Cα and Cβ groups differ in position by an average of 0.35 Å, following least-squares superposition of all protein Cα atoms. At the same time, the Cγ-carboxyl oxygen atoms superpose within 0.08–0.21 Å. Although the citrate molecule is slightly shifted with respect to isocitrate, this does not appear to be due to the absence of the Ser642 hydroxyl as in the S642A:isocitrate complex. Rather, the shift is toward Arg580, the

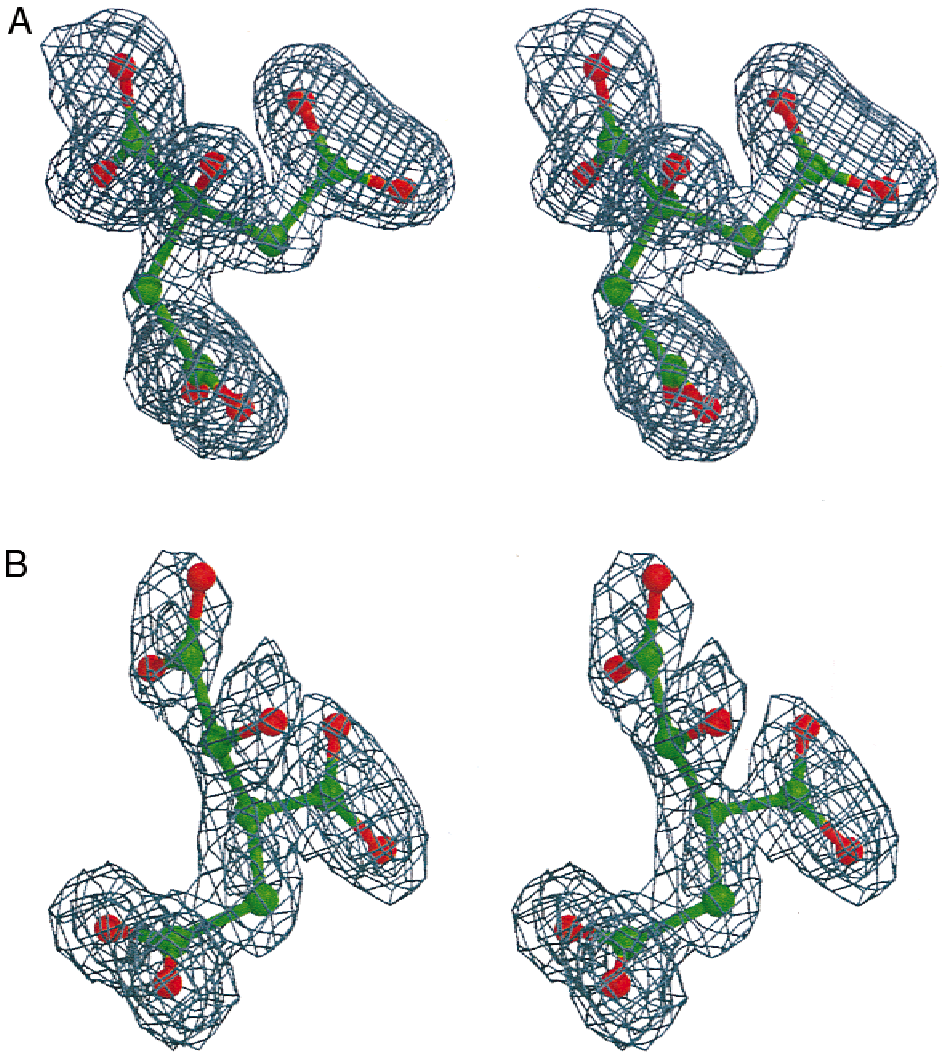

Fig. 2. Unbiased difference electron density for substrates bound to the S642A mutant of mitochondrial aconitase, confirming the citrate mode of binding in the catalytic mechanism. The maps are calculated using all data in the resolution range 20.0–1.8 Å for (**A**) the citrate complex, and in the resolution range 20.0–2.0 Å for (**B**) the isocitrate complex. Models for the substrates were not included in the structure factor calculations at any time prior to the computation of the electron density. The maps are computed with coefficients $|F_o| - |F_c|$ and contoured at 4.0 and 5.0 σ on a grid spacing of 25% of the maximum resolution.

residue involved in forming a salt bridge with the Cγ-carboxyl group (Fig. 3). The displacement may result from altered electrostatic interactions within the active site, due to the different angles of approach of the Cγ-carboxyl group (Fig. 4B). Importantly, the 0.35 Å shift of citrate would not change the length of the short contact to the Ser642 hydroxyl group, as judged by the distances from isocitrate Cβ to Ser642 Cβ, and citrate Cα to Ala642 Cβ, which remain the same (3.75 Å). Consequently, the positions of citrate and isocitrate equally favor the abstraction or addition of a proton by Ser642, as required in the catalytic mechanism (Fig. 1).

Materials and methods

Materials

All chemicals were obtained from Sigma (St. Louis, Missouri) (ACS grade) with the exception of the following: Isopropyl thio-β-D galactoside (IPTG; BioTech grade) was supplied by Fisher (Fair Lawn, New Jersey); Bactotryptone and Yeast Extract by Gibco (Gaithersburg, Maryland); ammonium sulfate (>99%) by Fluka (Milwaukee, Wisconsin); and Bradford's Reagent was obtained from BioRad Laboratories (Hercules, California). Reagents and supplies for gel electrophoresis were purchased from Novex (San Diego, California), and all chromatography resins from Pharmacia (Uppsala, Sweden). Fluorocitric acid was supplied by Dr. M.C. Kennedy, and plasmids encoding aconitase mutants were supplied by Dr. H. Zalkin.

Expression of recombinant aconitase in E. coli

Plasmid pAconitase (pA) encoding wild-type porcine mitochondrial aconitase (mAc) and plasmids pA (S642A) and pA (R644Q) encoding mutant enzymes (Zheng et al., 1992) were transformed into the *E. coli* strain BL21-DE3 by electroporation. Transformants

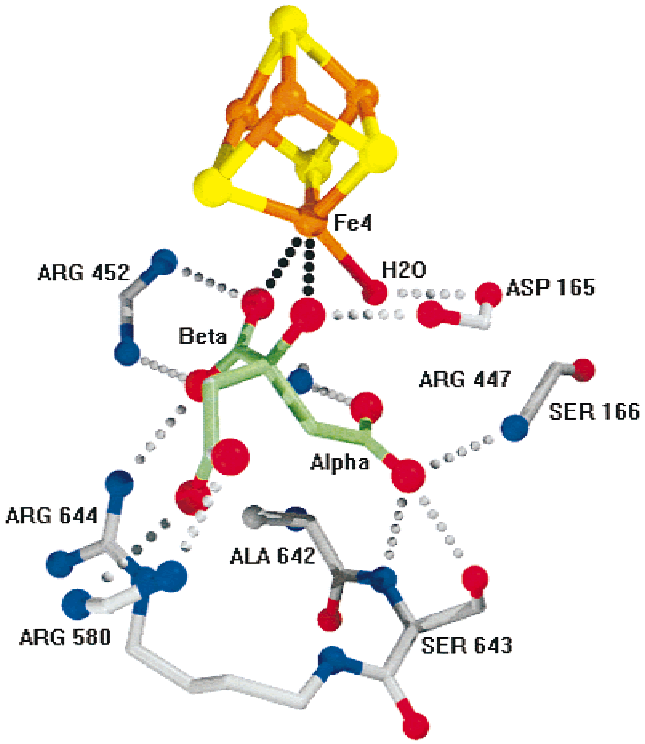

Fig. 3. The conformation of citrate bound to the S642A mutant of aconitase. The citrate hydroxyl and one Cβ-carboxyl oxygen are coordinated to Fe4 of the [4Fe-4S] cluster (Fe-O distances 2.59 and 2.37 Å, respectively; black dotted lines). There are 13 hydrogen bonds between citrate and the enzyme (gray dotted lines, 2.6–3.0 Å). Hydrogen bonds between the side chains of Gln72 and the Cγ-carboxyl group, Ser166 and the Cα-carboxyl group, and His101 and the hydroxyl group, are not shown for clarity.

were selected for ampicillin resistance and tested for the presence of the cloned gene by restriction analysis of the plasmid DNA. Cell stocks were prepared from single colonies by growing in L-Broth containing ampicillin (100 μg/mL) and freezing in liquid N_2 in the presence of 20% (v/v) glycerol.

Growth of cells and subsequent protein expression were carried out using a temperature-controlled shaker at 250 rpm. In a typical preparation *E. coli* cells expressing S642A or R644Q mAc were grown overnight at 37 °C in 6 × 20 mL cultures using 2 × YT medium containing ampicillin at 100 μg/mL. These cultures were then used to inoculate 6 × 200 mL of the same medium (prewarmed to 37 °C), and cell growth was continued for 4 h at 30 °C. Protein expression was induced by adding IPTG to a final concentration of 0.5 mM and aerating the cultures for a further 22–24 h at 30 °C. Synthesis of the 83 kD mutant enzymes was estimated by SDS-polyacrylamide gel electrophoresis (SDS-PAGE) to be 5–10% of the total soluble protein.

Protein purification

The [3Fe-4S] form was purified under aerobic conditions at 4 °C. All buffers were degassed under vacuum for ~20 min and prechilled to 4 °C before use. Purification was followed by SDS-PAGE combined with observation of the brown color of mAc. Cells were harvested (from a total of 1.32 L of culture) by centrifugation at 4,000 × *g* for 10 min. Cell pellets were resuspended on ice in 10 mM Tris-tricarballylate buffer (TTB), pH 7.0, containing 0.1 mM phenylmethane-sulfonyl fluoride (PMSF) in a final volume of 40 mL. The cell suspension was lysed by using a Sim-Aminco French Pressure cell at 16,000 psi (two passages), and the lysate cleared by centrifugation at 17,000 × *g* for 30 min.

Acidic proteins were removed from the supernatant by anion exchange using DEAE-Sepharose CL-6B. A 50% (v/v) slurry of this resin, pre-equilibrated in 10 mM TTB, pH 7.0 (60 mL) was added to the cleared lysate (~40 mL) and gently stirred for 20 min. The resin was removed by centrifugation at 2,000 × *g* for 10 min. The supernatant containing mAc was further purified by ammonium sulfate fractionation at 0 °C. The pH was maintained at 7.0 by the dropwise addition of 1 M NaOH. Solid ammonium sulfate was slowly added with stirring to 50% saturation, the extract was stirred gently for 15 min, incubated on ice for 15 min, and centrifuged at 27,000 × *g* for 30 min. The supernatant containing mAc was removed, brought to 80% ammonium sulfate saturation, stirred gently for 30 min, and incubated on ice for 30 min. Precipitated protein including mAc was pelleted as above.

Purification of S642A mutant

Precipitated protein was resuspended in 10 mM TTB, pH 7.0 containing 0.25 M NaCl and 0.05% (v/v) Triton X-100 and dialyzed overnight against 2 L of this buffer. The brown solution was applied to a Sephacryl-200 HR column (1.5 × 90 cm) pre-equilibrated with the above buffer. Gel filtration was performed at a flow rate of 5.0 mL/h under gravity. Fractions (1.5 mL) were collected over a period of 24–26 h until the brown aconitase was eluted. Pooled fractions were concentrated in an Amicon stirred ultrafiltration cell under N_2 at 60 psi using a YM-30 membrane. The buffer solution was exchanged by adding 3 × 10 mL of 60 mM TTB, pH 7.8. The concentrated protein (~2.0 mL at 18 mg/mL) was transferred to an anaerobic hood (<1 ppm O_2) and stored at 4 °C.

Purification of R644Q mutant

Precipitated protein was resuspended in 10 mM TTB, pH 7.0 containing 0.25 M NaCl. The protein solution was dialyzed overnight against 2 × 2 L of this buffer and applied to a Sephacryl-200 HR column (2.5 × 90 cm) equilibrated in the same buffer. The column was washed at 15 mL/h under gravity, and fractions (4.5 mL) were collected, pooled, and concentrated as for the S642A mutant. The protein solution was brought to 1.0 M NaCl by the addition of 5 M NaCl, mixed gently, incubated on ice for 5 min, and applied to a Phenyl-Sepharose CL-4B column (1.5 × 7.0 cm; 10 cm^3 volume) pre-equilibrated with 10 mM TTB, pH 7.0 in 1.0 M NaCl. The column was washed with 3.5 column volumes of equilibration buffer. The protein was eluted with a linear, decreasing sodium chloride gradient (12 mL/h) consisting of 100 mL of 10 mM TTB, pH 7.0, in 1.0 M NaCl, and an equal volume of buffer in 0.6 M NaCl. Aconitase fractions (1.1 mL) were collected, pooled, concentrated, and buffer exchanged as described for S642A mAc. The concentrated protein (~0.7 mL at 18 mg/mL in 60 mM TTB, pH 7.8) was transferred to the anaerobic hood and stored at 4 °C.

Reconstitution

A_{400}/A_{280} measurements of the samples showed that 45–65% of the total protein was in the [3Fe-4S] form relative to native acon-

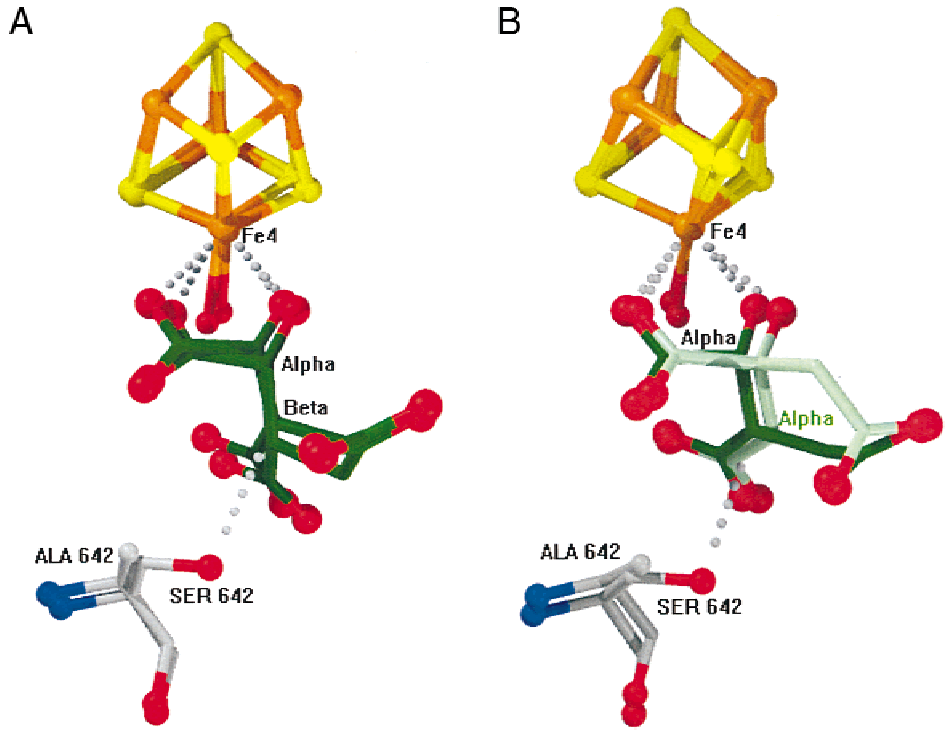

Fig. 4. Superposition of isocitrate and citrate complexes of aconitase. **A:** The isocitrate complexes (dark green) with the native enzyme (Ser642) and the S642A mutant (Ala642) showing that the mutation has not altered the mode of binding, although isocitrate shifts away slightly from the [4Fe-4S] cluster in the mutant enzyme. The positions of the Cα and Cβ atoms are indicated. **B:** The isocitrate complex (dark green) with the native enzyme (Ser642) and the citrate complex (light green) with the S642A mutant (Ala642) showing that the two substrates bind with their Cα–Cβ bonds inverted with respect to each other. The substrates coordinate to Fe4 in a similar manner, and their Cγ-carboxyl groups superpose. The Cα atoms of isocitrate (black label) and citrate (green label) are indicated. A short contact between Cβ of isocitrate and Ser642 is indicated in both figures.

itase (Emptage et al., 1983). Reconstitution was done at room temperature under anaerobic conditions as described previously (Kennedy & Beinert, 1988) with modifications. The protein concentration was 0.2 mM and ferrous ammonium sulfate and sodium sulfide were added in 10-fold excess. Dithiothreitol (DTT) was added in 50-fold excess. After 4 h NaCl was added to 1.0 M and the mixture was allowed to stand for 5 min. NaCl (1.0 M) was required for separation of the protein from colloidal ferrous sulfide formed as a by-product of the reconstitution procedure.

Reconstituted mAc was separated from ferrous sulfide using Octyl-Sepharose CL-4B under aerobic conditions at 4 °C within 5 min of removal from the anaerobic hood. The protein solution was applied under gravity to a 5.0 cm^3 column pre-equilibrated with 10 mM TTB, pH 7.0, containing 1.0 M NaCl, and was eluted with two column volumes; black ferrous sulfide remained bound to the column. The protein solution (6–10 mL) was mixed gently, left on ice for 5 min to allow oxidation of residual ferrous sulfide, concentrated and buffer exchanged by ultrafiltration under N_2 with 3×10 mL of 60 mM TTB, pH 7.8. During ultrafiltration a trace of oxidized by-product (reddish color, Fe^{3+}) was observed in the filtrate. Concentrated protein samples (0.5–1.0 mL at 18–20 mg/mL) were returned to the anaerobic hood and stored at 4 °C.

Analysis of purified enzymes

S642A mAc was approximately 90% pure by SDS-PAGE and was 100% in the [3Fe-4S] form based on the A_{400}/A_{280} measurements (Emptage et al., 1983). The yield was typically 15 mg from 1.32 L of culture. R644Q aconitase was >95% pure by SDS-PAGE and was also 100% in the [3Fe-4S] form. The yield was typically 9–11 mg from 1.32 L of culture. Expression, purification, and reconstitution required a total of six to seven days.

Protein crystallization

Purified, reconstituted samples of S642A and R644Q mAc in the [3Fe-4S] form were diluted to 16–18 mg/mL protein using degassed sample buffer (60 mM TTB, pH 7.8). Reactivation of the mutant enzymes to the [4Fe-4S] form and subsequent crystallization used established procedures (Lauble et al., 1992) with modifications. Reservoir solutions were in the range 2.2 to 2.4 M ammonium sulfate in 0.25 M Bis-Tris-HCl, 0.35 M NaCl, pH 7.0. Drops were prepared by mixing 12 μL of the protein solutions with 16–18 μL of saturated ammonium sulfate in 0.25 M Bis-Tris-HCl and 0.35 M NaCl, pH 7.0. Nucleation was induced by streak-seeding (Stura & Wilson, 1990) using crystals of native or mutant mAc. Crystals were grown under anaerobic conditions for four to eight weeks at 26 °C.

Co-crystallization

Three structures of mAc mutants were determined in which a mutant enzyme was incubated with substrate or inhibitor during

crystallization. The compounds were added to protein solutions to 10 mM using 200 mM stock solutions, and the solutions were allowed to stand for 10 min prior to mixing with ammonium sulfate for crystallization. Each structure was refined at 2.5 Å resolution (data not shown). The structure of the S642A mutant incubated with *cis*-aconitate revealed electron density consistent with isocitrate, showing that this kinetically most impaired mutant is able to turn over during cocrystallization. The structure of the R644Q mutant (V_{max} 0.25–0.46 relative to the native enzyme) incubated with fluorocitrate revealed density consistent with fluorocitrate, indicating that a marginally impaired mutant is not able to turn over an inhibitor. Consequently, the structure of the S642A mutant cocrystallized with fluorocitrate also showed density consistent with the citrate mode. These experiments are consistent with the kinetic properties of the mutants, and they support the existence of the citrate mode. However, they demonstrate that it is not possible to capture a complex of citrate itself by co-crystallization.

Soaking

For soaking experiments, crystals were transferred to a synthetic mother liquor of 2.8 M ammonium sulfate in 0.2 M Bis-Tris-HCl, 0.28 M NaCl, pH 7.0 containing 40 mM substrate or inhibitor and 1 mM sodium dithionite, and soaked for one to four days at 26 °C. As shown by the results (Fig. 2A,B), the S642A mutant is unable to turn over either citrate or isocitrate when the enzyme is restrained in the crystal lattice, at least on the time scale of ≤4 days.

Data collection

Data were collected at Stanford Synchrotron Radiation Laboratory beam line 7-1 (λ 1.08 Å) at 100 K by flash freezing crystals in a N_2 gas stream using a cryo-protectant consisting of 15% glycerol in the synthetic mother liquor. Data were recorded with a Mar345 imaging plate using 1° oscillations. Data were collected for crystals of the S642A mutant soaked in citrate, isocitrate, *cis*-aconitate, *trans*-aconitate, and fluorocitrate. The data were indexed, integrated, merged, and scaled with Mosflm and the CCP4 suite of programs (Leslie, 1994). Only the crystals soaked in citrate and isocitrate displayed diffraction to ≤2.0 Å resolution (Table 1).

Structure refinement

The S642A mAc complexes were solved by molecular replacement using the structure of the native enzyme as a starting model (Robbins & Stout, 1989). Coordinates for the reference native mAc structure were edited to omit the [4Fe-4S] cluster, any bound species and all H_2O molecules, and residue 642 was modeled as Gly. The models were subjected to rigid body refinement using X-PLOR (version 3.8) (Brünger et al., 1989) in increasing steps of resolution until all data were incorporated. Positional parameters and isotropic *B*-factors were refined by simulated annealing with inclusion of a bulk solvent correction. Unbiased $|F_o| - |F_c|$ maps were used to model the [4Fe-4S] cluster and confirm the presence of Ala642, and $2|F_o| - |F_c|$ maps were used to check and adjust the fit to the electron density of the 753 additional amino acids. The XtalView suite of programs was used for all model and map manipulations (McRee, 1999a). The models were subjected to four to five subsequent rounds of refinement in which $|F_o| - |F_c|$ and $2|F_o| - |F_c|$ maps were used to interpret the sites of solvent molecules, including H_2O bound to Fe4 of the [4Fe-4S] cluster.

Following convergence of this process, unbiased $|F_o| - |F_c|$ maps were computed to interpret the electron density for the bound substrates. The 4.0–5.0σ density for the citrate-soaked crystal at 1.8 Å resolution clearly revealed the positions of the Cα and Cγ atoms linked to the central Cβ atom of citrate carrying the hydroxyl group (Fig. 2A). Similarly, the unbiased 4.0–5.0σ density for the isocitrate soaked crystal was clearly recognizable as that of isocitrate due to density for the branching hydroxyl group on Cα and connecting density between Cβ and Cγ (Fig. 2B). Citrate and isocitrate were modeled using the nitrocitrate and isocitrate complexes of the native enzyme as guides (Lauble et al., 1992, 1994). The structures were refined with the substrates included, and $2|F_o| - |F_c|$ and $|F_o| - |F_c|$ maps were inspected to confirm the fit of the models to the density. Refinement statistics are summarized in Table 1.

Ramachandran plots for the S642A mAc structures show that in each case 98.9% of 681 nonglycine residues are in the most favored or allowed regions: four of seven nonglycine outliers, Thr229, Ser357, Ala573, and Asp635, have low *B*-factors and exhibit strong density; the remaining three have high *B*-factors. Coordinates of the S642A:citrate and S642A:isocitrate complexes (Table 1) have been deposited with the Protein Data Bank, accession codes 1C96 and 1C97, respectively. In addition, the coordinates for mutant mAc complexes prepared by cocrystallization and refined at 2.5 Å resolution (data not shown) have been deposited with the Protein Data Bank: S642A:isocitrate, S642A:fluorocitrate and R644Q: fluorocitrate; accession codes 1AR3, 1AS9 and 1ATQ, respectively. Figure 2 was rendered with Raster3d (Merritt & Murphy, 1994), and Figures 3 and 4 were prepared using Molw and Showcase (McRee, 1999b).

Acknowledgments

We thank H. Zalkin for the generous gift of plasmids encoding mAc mutants; M.C. Kennedy for advice regarding [Fe-S] reconstitution; E.A. Stura, D.B. Goodin, G. Jensen, J.F. Harper, and S.P. Mayfield for technical advice regarding crystallization, [Fe-S] cluster chemistry, and protein expression. This work supported by National Institutes of Health Grants GM48495 and GM36325.

References

Beinert H, Kennedy MC, Stout CD. 1996. Aconitase as iron-sulfur protein, enzyme, and iron-regulatory protein. *Chem Rev 96*:2335–2373.

Beinert H, Kiley P. 1996. Redox control of gene expression involving iron-sulfur proteins. Change of oxidation-state or assembly/disassembly of Fe-S clusters? *FEBS Lett 382*:218–219.

Brünger AT, Karplus M, Petsko GA. 1989. Crystallographic refinement by simulated annealing: Application to crambin. *Acta Crystallogr A45*:50–61.

Emptage MH. 1988. Aconitase: Evolution of the active-site picture. In: Que L Jr, ed. *Metal clusters in proteins*. ACS Symp. Series 372. Washington, DC: American Chemical Society. pp 343–371.

Emptage MH, Dreyer J-L, Kennedy MC, Beinert H. 1983. Optical and EPR characterization of different species of active and inactive aconitase. *J Biol Chem 258*:11106–11111.

Flint DH, Allen RM. 1996. Iron-sulfur proteins with nonredox functions. *Chem Rev 96*:2315–2334.

Flint DH, Emptage MH, Finnegan MG, Fu W, Johnson MK. 1993. The role and properties of the iron-sulfur cluster in *Escherichia coli* dihydroxy-acid dehydratase. *J Biol Chem 268*:14732–14742.

Green J, Bennett B, Jordan P, Ralph ET, Thomson AJ, Guest JR. 1996. Reconstitution of the [4Fe-4S] cluster in FNR and demonstration of the aerobic-anaerobic transcription switch *in vitro*. *Biochem J 316*:887–892.

Haile DJ, Rouault TA, Harford JB, Kennedy MC, Blondin GA, Beinert H, Klausner RD. 1992. Cellular regulation of the iron-responsive element binding protein: Disassembly of the cubane iron–sulfur cluster results in high-affinity RNA binding. *Proc Natl Acad Sci USA 89*:11735–11739.

Kennedy MC, Beinert H. 1988. The state of cluster SH and S^{2-} of aconitase during cluster interconversions and removal. *J Biol Chem 263*:8194–8198.
Kennedy MC, Stout CD. 1992. Aconitase: An iron-sulfur enzyme. *Adv Inorg Chem 38*:323–339.
Kent TA, Emptage MH, Merkle H, Kennedy MC, Beinert H, Münck E. 1985. Mössbauer studies of aconitase. *J Biol Chem 260*:6871–6881.
Khoroshilova N, Popescu C, Münck E, Beinert H, Kiley PJ. 1997. Iron–sulfur cluster disassembly in the FNR protein of *Escherichia coli* by O_2: [4Fe-4S] to [2Fe-2S] conversion with loss of biological activity. *Proc Natl Acad Sci USA 94*:6087–6092.
Lauble H, Kennedy MC, Beinert H, Stout CD. 1992. Crystal structures of aconitase with isocitrate and nitroisocitrate bound. *Biochemistry 31*:2735–2748.
Lauble H, Kennedy MC, Beinert H, Stout CD. 1994. Crystal structures of aconitase with *trans*-aconitate and nitrocitrate bound. *J Mol Biol 237*:437–451.
Lazazzera BA, Beinert H, Khoroshilova N, Kennedy MC, Kiley PJ. 1996. DNA binding and dimerization of the Fe-S-containing FNR protein from *Escherichia coli* are regulated by oxygen. *J Biol Chem 271*:2762–2768.
Leslie AGW. 1994. The CCP4 suite: Programs for protein crystallography. *Acta Crystallogr D50*:760–763.
McRee DE. 1999a. XtalView/Xfit—A versatile program for manipulating coordinates and electron density. *J Struct Biol 125*:156–165.
McRee DE. 1999b. *Molecular images software*. San Diego, California.
Merritt GA, Murphy MGP. 1994. Raster 3D version 2.0: A program for photorealistic molecular graphics. *Acta Crystallogr D50*:869–873.
Robbins AH, Stout CD. 1989. Structure of activated aconitase: formation of the [4Fe-4S] cluster in the crystal. *Proc Natl Acad Sci USA 86*:3639–3643.
Rouault TA, Klausner RD. 1996. Iron–sulfur clusters as biosensors of oxidants and iron. *Trends Biosci 21*:174–177.
Rouault TA, Stout CD, Kaptain S, Harford JB, Klausner RD. 1991. Structural relationship between an iron-regulated RNA-binding protein (IRE-BP) and aconitase: Functional implications. *Cell 64*:881–883.
Schloss JV, Emptage MH, Cleland WW. 1984. pH profiles and isotope effects for aconitases from *Saccharomycopsis lipolytica*, beef heart, and beef liver. α-methyl-*cis*-aconitate and *threo*-D_s-α-methylisocitrate as substrates. *Biochemistry 23*:4572–4580.
Skala J, Capieaux E, Balzi E, Chen WN, Goffeau A. 1991. Complete sequence of the *Saccharomyces cerevisiae* LEU1 gene encoding isopropylmalate isomerase. *Yeast 7*:281–285.
Stura EA, Wilson IA. 1990. Analytical and production seeding techniques. *Methods Companion Methods Enzymol 1*:38–49.
Zheng L, Andrews PC, Hermodson MA, Dixon JE, Zalkin H. 1990. Cloning and structural characterization of porcine heart aconitase. *J Biol Chem 265*:2814–2821.
Zheng L, Kennedy MC, Beinert H, Zalkin H. 1992. Mutational analysis of active site residues in pig heart aconitase. *J Biol Chem 267*:7895–7903.